Detailed mapping of biaxial orientation in polyethylene terephthalate bottles using polarised attenuated total reflection FTIR spectroscopy

Matthew R. Smith [a], Sharon J. Cooper [a,*], Derek J. Winter [b], Neil Everall [c]

[a] Department of Chemistry, University of Durham, Durham DH1 3LE, UK
[b] INVISTA Performance Technologies, Wilton, Redcar, Cleveland TS10 4XX, UK
[c] ICI Measurement Science Group, The Wilton Centre, Wilton, Redcar TS10 4RF, UK

Abstract

Polarised attenuated total reflection FTIR spectroscopy has been used for detailed orientation mapping of 2l polyethylene terephthalate bottles subjected to different preform heating times. The results for the bottle with the standard preform heating time reveal significant surface orientation variations along the bottle hoop and length directions, with the inner bottle surface also showing consistently greater chain orientation in the hoop direction than found for the outer surface. Decreasing the preform heating time has less effect on the chain orientation than increasing the heating time, with the latter causing reduced chain orientation in the final bottle. The absorbance of the 1340 cm^{-1} band provides a quick and reliable indication of these chain orientation trends. In contrast, the extent of benzene ring orientation parallel to the bottle surface showed little variation and remained consistently high at the majority of the surface bottle positions probed.
© 2006 Elsevier Ltd. All rights reserved.

1. Introduction

Polarised attenuated total reflection (ATR) FTIR is a versatile technique that can be used to characterise the near surface biaxial orientation in artefacts that are too thick for transmission IR experiments and are too highly curved to provide accurate X-ray incidence angles for X-ray diffraction orientation studies. The technique involves holding a polymer surface in intimate contact with an IR-transmitting prism, the ATR element, and controlling the IR beam polarisation state. The ATR element has a high refractive index to ensure that total internal reflection occurs, so that the IR beam probes the near surface of the polymer. Although anomalous dispersion in ATR can distort the resulting band intensities to different degrees for different IR polarisations, this effect is minimised for a high refractive index ATR element, such as germanium. In addition, effects due to different sample-prism contact areas are eliminated by using a band normalisation method, and the analysis becomes less sensitive to the exact value of the polymer

refractive index, so that a typical intermediate value can reliably be assumed [1]. This enables an accurate description of the relative biaxial orientation of the polymer surface to be obtained, provided a linear relationship between concentration and ATR absorbance is found. For PET, this condition is met, and good agreement between the ATR technique and specular reflectance and birefringence studies is generally found [1]. Consequently, although there are many detailed and informative X-ray diffraction studies on PET [2], polarised FTIR-ATR remains the most practical method of obtaining relative biaxial orientation measurements on the surfaces of thick and irregularly shaped samples. Polarised FTIR-ATR employing this band normalisation technique has recently been successfully applied to the panel and shoulder regions of the outer and inner surfaces of stretch-blown PET bottles and has revealed substantial orientation gradients both along the bottle length and through the bottle thickness [3]. The present work aims to explore the nature of the chain orientation in greater detail by mapping the near-surface orientation at regular 2 cm intervals along the inner and outer walls of 2l stretch-blown PET bottles that have been subjected to different preform heating times, see Fig. 1. The orientation of the benzene ring relative to the bottle surface is addressed, as well as the chain orientation. Furthermore, we also assess the suitability of using the

---

* Corresponding author. Tel.: +44 191 374 4638.
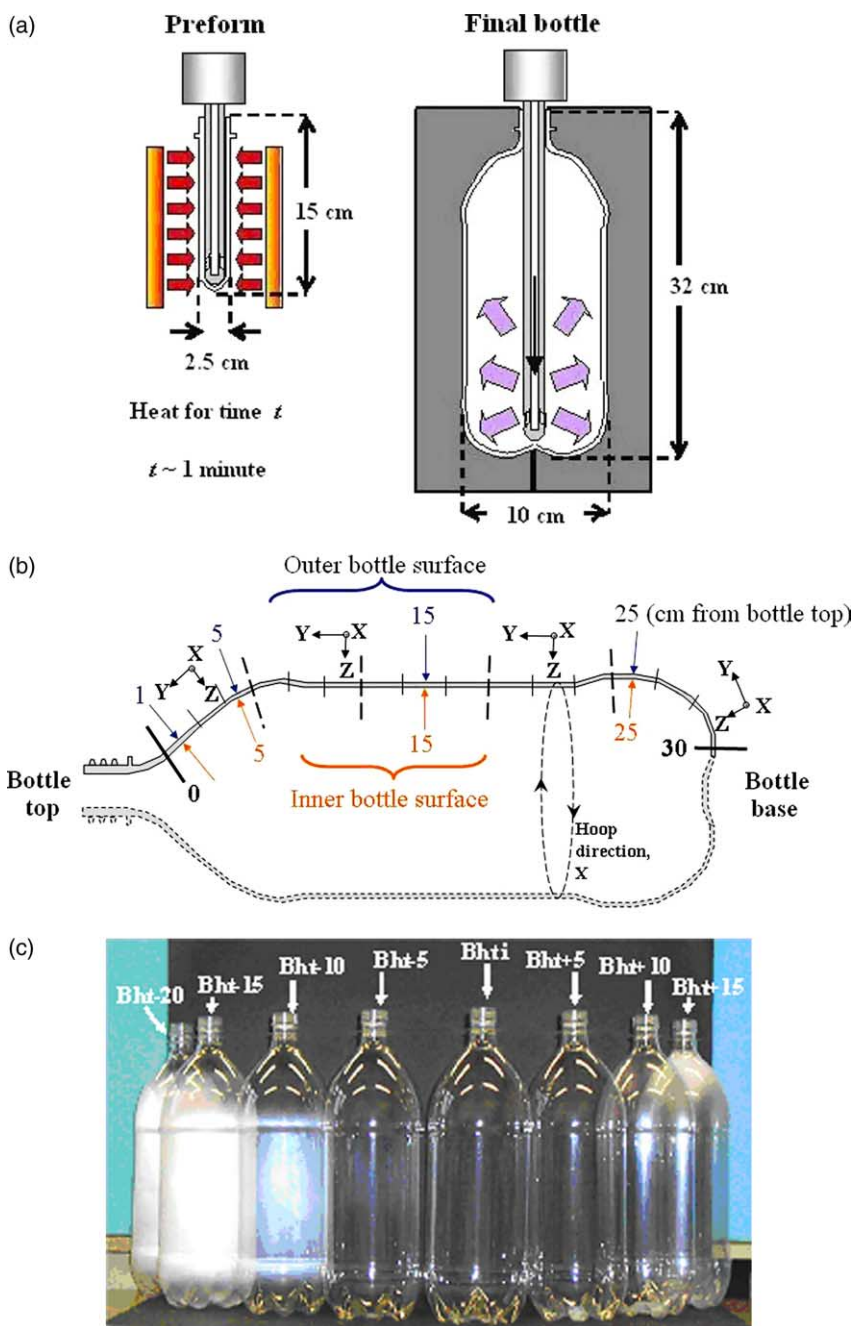E-mail address: sharon.cooper@durham.ac.uk (S.J. Cooper).

Fig. 1. (a) A schematic diagram of the stretch-blow process used in PET bottle manufacture. (b) Relating the *X*, *Y*, *Z* sample directions to the positions probed on the bottle. Note that the minimum bottle wall thickness (240 μm) is much greater than the ATR sampling depth ($\sim$1–2 μm), which allows the orientation along the inner and outer bottle surfaces to be mapped independently. (c) A photograph of the Bht series of 2*l* PET bottles.

absorbance of the 1340 cm^{-1} CH$_2$ wag mode of the *trans* ethylene glycol conformer as a simple chain orientation indicator. This parallel band, with $\beta = 21°$ [4,5], has previously been used to measure crystallinity [6–9].

2. Experimental

2.1. Uniaxially drawn PET films

Uniaxially drawn films of thickness $\sim$150 μm were used to compare the orientation results obtained from X-ray diffraction

and polarised FTIR-ATR analysis. The films were produced at DuPont Teijin Films, Wilton UK, on a 'Long stretcher', which has the facility to heat the samples and stretch them uni- or biaxially up to draw ratios of four.

2.2. Bottle production conditions

The bottles were produced from a stretch-blow moulding process in which a heated preform is simultaneously stretched with a stretch rod and blown up with high pressure air to fill a mould with the desired bottle shape. The preform was heated

by 10 IR heaters with a total output of 25 kW, which were distributed along the length of the preform. The 10 heaters, positioned from the preform bottom to the top, were set to be 'on' for a percentage of the total heat time, t, as follows. 86, 86, 96, 96, 22, 22, 24, 24, 85 and 90%. Providing more heat at the top and the bottom of the preform ensures increased polymer flow and ultimately more material at the bottle top and base. For a standard bottle, the total heat time, t, was 44 s. After the heaters are turned off, there is a delay of 10 s to allow partial temperature equilibration, which is promoted by re-radiation of heat from the Sb IR absorber present in the polymer. The outer surface temperature of the preform is then ∼ 110–115 °C. The mould is then closed around the preform and the primary air blowing step begins with 0.7 s of air at 10–12 bar. 0.2 s after the primary air blow, the stretch rod drives up the centre of the preform. The secondary air blow lasts for 2.5 s and uses air at 30 bar to ensure that the required bottle shape is achieved through full contact with the mould. This operation was performed on a relatively old rig, however, modern stretch blowing kits would follow a similar procedure albeit at a quicker rate.

2.3. X-ray diffraction

X-ray diffraction studies on the uniaxially drawn PET films were conducted on a D8 Bruker diffractometer with a 2D multiwire detector at a fixed X-ray incidence angle of 5° to provide a depth penetration comparable to that of the ATR technique. In the PET crystalline regions, the chain lies nearly perpendicular to the $\bar{1}05$ direction, with

$$\langle \cos^2 \sigma_{\bar{1}05} \rangle = 1 - 0.3481 \langle \cos^2 \sigma_{100} \rangle - 0.8786 \langle \cos^2 \sigma_{010} \rangle$$

$$- 0.7733 \langle \cos^2 \sigma_{\bar{1}10} \rangle.$$

Hence we find $\langle \cos^2 \sigma_{hkl} \rangle$ for each of the 100, 010 and 110 diffraction signals by using

$$\langle \cos^2 \sigma_{hkl} \rangle = \int_0^{\pi/2} I_{hkl} \sin\phi \cos^2\phi \, \mathrm{d}\phi \Big/ \int_0^{\pi/2} I_{hkl} \sin\phi \, \mathrm{d}\phi$$

, where I_{hkl} is the measured intensity of the (hkl) signal at the angle ϕ, and then set $\langle \cos^2(yY) \rangle = \langle \cos^2 \sigma_{\bar{1}05} \rangle$.

2.4. Polarised FTIR-ATR

Polarised FTIR-ATR measurements were collected using a ZnSe polariser and a single-bounce Thunderdome (Spectra-Tech) ATR accessory in the sample chamber of a Nicolet Nexus spectrometer, equipped with a liquid nitrogen cooled HgCdTe detector. The Thunderdome ATR accessory incorporates a germanium internal reflection element with a fixed incident angle of 45° and ∼ 1 mm² contact area; samples are clamped to the germanium ATR element using a fixed torque anvil. The germanium ATR element has a refractive index of 4, so the evanescent IR field probes ∼ 1–2 μm into the PET bottle surface for wavenumbers in the relevant range of 1700–850 cm⁻¹. 32 scans at 2 cm⁻¹ spectral resolution were
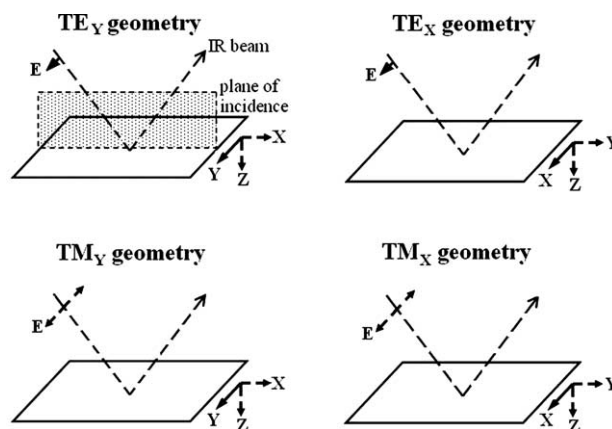

Fig. 2. The four geometries obtained using an IR polariser.

acquired for each spectrum. The spectra were ratioed against the appropriate polarised background spectrum, taken prior to the sample data collection.

The IR beam was polarised either parallel (TM) or perpendicular (TE) to the plane of incidence, whilst the sample was aligned with either the X or Y principal axis aligned perpendicular to the plane of incidence, see Fig. 2. This provided four sets of spectra for each bottle sample position, denoted TM$_X$, TM$_Y$, TE$_X$ and TE$_Y$. This process was repeated at every mapping point from the top to the bottom of the bottle for the outer bottle surface, with fresh backgrounds recorded at the start of each group of four spectra. The whole process was repeated for the inner bottle wall of the same sample strip at the corresponding positions to those studied for the outer wall. Excellent reproducibility (∼2%) was found in the value of the 1340 cm⁻¹ peak height in 10 repeated measurements taken at a random bottle position, and so we consider the largest error in our absorbance measurements arises from the baseline fitting, for which an error of 6% was obtained on using a range of sensible baselines. Consequently, the absorbance measurements were conservatively estimated to be accurate to within 10%. For the most highly oriented surface regions that have $\langle \cos^2(jX) \rangle$ values above 0.9, this produces a maximum possible error [10] of 0.14 in the $\langle \cos^2(jJ) \rangle$ values. However, maximum error values of 0.09 or lower are more typical of other surface regions with $\langle \cos^2(jJ) \rangle$ values of 0.6 or less.

2.5. Theory

The biaxial orientation of the PET bottles was assessed by using P_{lmn} orientation parameters to determine the average square direction cosine, $\langle \cos^2(jJ) \rangle$, where jJ denotes the angle between the PET molecular axis j and the sample axis J. $J = X$, Y and Z denotes the bottle hoop, length and thickness directions, respectively, see Fig. 1(b), whilst $j = x$, y and z denotes the directions along the PET chain, perpendicular to the PET chain (in the plane of the benzene ring), and perpendicular to both the PET chain and the benzene ring. The equations relating the P_{lmn} orientation parameters to the

$\langle\cos^2(jJ)\rangle$ values pertinent to this study are as follows [11]

$$\langle\cos^2(yY)\rangle = \frac{1}{3} + \frac{2}{3}P_{200},$$

$$\langle\cos^2(yX)\rangle = \frac{1}{3} - \frac{1}{3}P_{200} + 2P_{220},$$

$$\langle\cos^2(yZ)\rangle = \frac{1}{3} - \frac{1}{3}P_{200} - 2P_{220},$$

$$\langle\cos^2(zZ)\rangle = \frac{1}{3} + \frac{1}{6}P_{200} - P_{220} + P_{202} + P_{222},$$

$$\langle\cos^2(zX)\rangle = \frac{1}{3} + \frac{1}{6}P_{200} - P_{220} + P_{202} - P_{222} \text{ and}$$

$$\langle\cos^2(zY)\rangle = \frac{1}{3} - \frac{1}{3}P_{200} - 2P_{202}.$$

The P_{lmn} orientation parameters were determined by measuring the absorbance of the $1017\,\mathrm{cm}^{-1}$ ($\sim$parallel) band, for which the angle, β, between the chain and transition dipole is $\sim 20°$, and the $875\,\mathrm{cm}^{-1}$ ($\sim$perpendicular) band for which $\beta \sim 85°$ in each of the TM_X, TM_Y, TE_X and TE_Y geometries. The 1017 and $875\,\mathrm{cm}^{-1}$ bands are well-characterised ring vibrations, so the values of β are well known from previous work [12]. The use of these bands allows the benzene ring orientation parallel to the bottle surface to be assessed readily through the $\langle\cos^2(zZ)\rangle$ parameter, whilst the chain orientation is indicated by $\langle\cos^2(yY)\rangle$. The band intensities were normalised relative to the $1410\,\mathrm{cm}^{-1}$ band, in order to correct for differing contact areas and pressures in moving from the TE to TM configurations. The intensity of the $1410\,\mathrm{cm}^{-1}$ band is known [13] to be non-dichroic and independent of crystallinity up to a draw ratio of 4. Furthermore, its use as a normalisation band has already been successfully demonstrated [1,3]. The P_{lmn} orientation parameters were then extracted from the normalised 1017 and $875\,\mathrm{cm}^{-1}$ band intensities using the method of Everall and Bibby [1,3]. The successful use of similar FTIR-ATR spectroscopy approaches in determining orientation in many polymers has previously been reported [14].

3. Results

3.1. Validation of polarised FTIR-ATR numerical data

The bottle sections were too highly curved to obtain accurate biaxial orientation information from X-ray diffraction

studies, so we used uniaxially drawn PET films to compare $\langle\cos^2(yY)\rangle$ values obtained from the polarised FTIR-ATR technique and X-ray diffraction, the latter though only provide the chain orientation within the crystalline regions. Table 1 shows that we obtain excellent agreement between the two techniques, suggesting that the quantitative biaxial measurements obtained using polarised FTIR-ATR are reliable.

3.2. PET bottle with the standard preform heating

The $\langle\cos^2(yJ)\rangle$ values along the length of a bottle with the standard preform heating are presented graphically in Fig. 3. The $\langle\cos^2(yZ)\rangle$ values are consistently low ($\sim$0–0.1) for all bottle positions, implying very low chain orientation in the thickness direction for the surface region, and so to a first approximation the surface chain orientation can be described by considering only the $\langle\cos^2(yX)\rangle$ and $\langle\cos^2(yY)\rangle$ values, i.e. the in-plane parameters. For the outer bottle surface, the bottle neck surface contains chains oriented predominately along the bottle length (Y direction). Over the shoulder of the bottle, the proportion of chains lying in the bottle length (Y) direction decreases at approximately the same rate that the orientation in the hoop (X) direction begins to increase. At 7 cm from the bottle top, the $\langle\cos^2(yY)\rangle$ and $\langle\cos^2(yX)\rangle$ values are similar, implying balanced biaxial orientation. Further down the bottle wall, the number of chains in the surface hoop direction begins to dominate, resulting in an outer-wall surface orientation maximum in the hoop direction at 25 cm from the bottle top. This $\langle\cos^2(yX)\rangle$ maximum coincides with a minimum in both the $\langle\cos^2(yY)\rangle$ and $\langle\cos^2(yZ)\rangle$ values, the latter showing that the biaxial orientation is at a maximum, which presumably arises due to the combined effects of a maximal preform hoop extension and maximal preform heating time of 42 s for this location. The surface base region then shows a downturn in the $\langle\cos^2(yX)\rangle$ value to the last sampling region under the foot of the bottle, where the number of surface chains oriented along the bottle length and hoop directions are similar.

The inner surface wall of the bottle (see Fig. 3(b)) shows similar orientation trends, although the extent of hoop-direction surface chain orientation is higher throughout. At 1 cm from the bottle top, the number of surface chains lying along the bottle length dominates in a similar fashion to the outside wall. However, the switch between predominantly bottle-length direction surface chains to predominantly hoop-direction surface chains occurs much higher, at 3 cm from the bottle top. The number of surface chains in the hoop direction then dominates for the rest of the bottle except for the base,

Table 1
Comparison of $\langle\cos^2(yY)\rangle$ values obtained for uniaxially drawn PET film from X-ray diffraction and polarised FTIR-ATR analysis

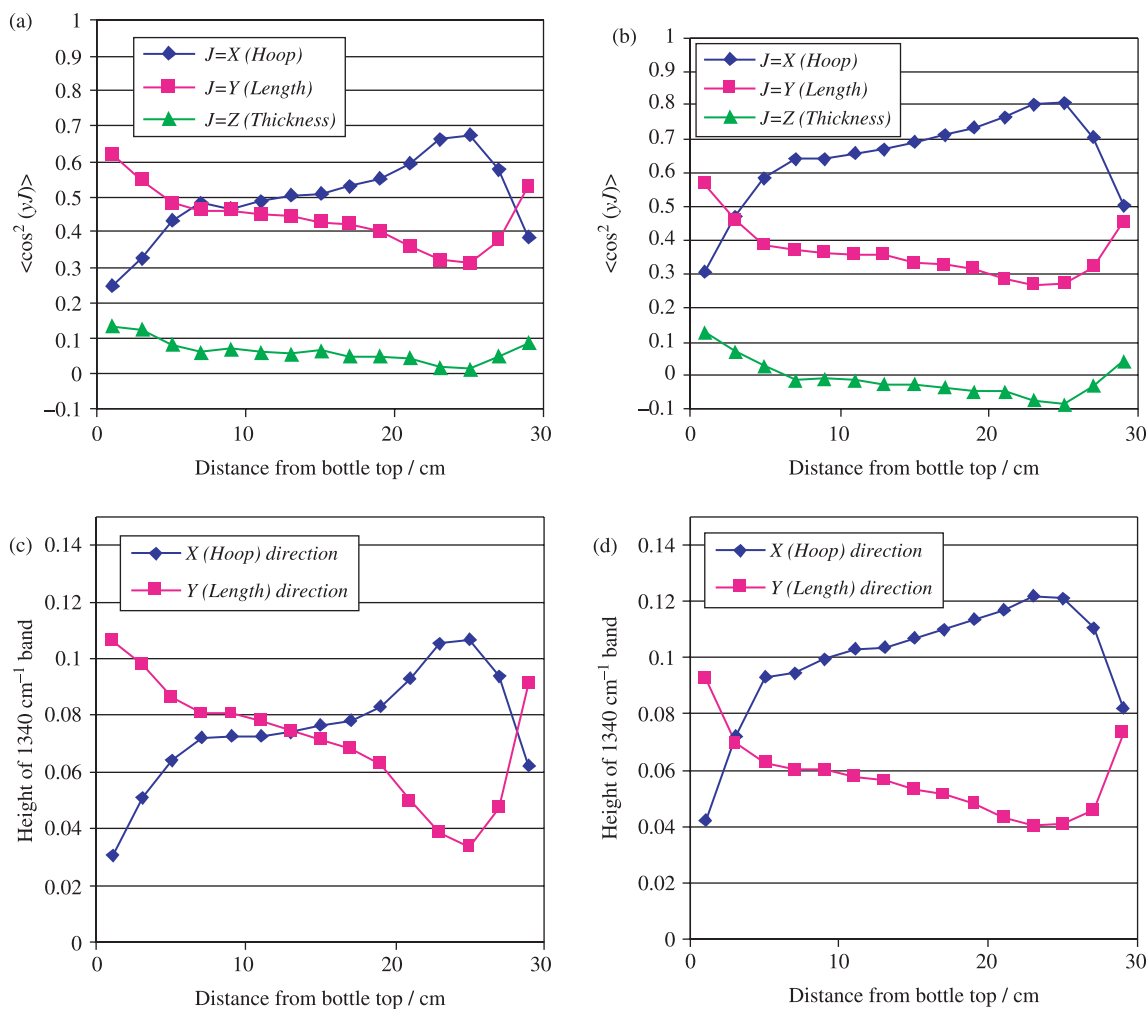| Film draw ratio	3.75	3.75	3.75	3.75	3.00
Annealing conditions	None	200 °C for 5 min	200 °C for 60 min	200 °C for 75 min	200 °C for 75 min
X-ray diffraction $\langle\cos^2(yY)\rangle$	0.73	0.76	0.77	0.76	0.76
Polarised FTIR-ATR $\langle\cos^2(yY)\rangle$	0.70	0.77	0.77	0.75	0.77

Fig. 3. Chain orientation results for a standard PET bottle (Bht) along the bottle length. (a) Outer surface $\langle\cos^2(yJ)\rangle$ values. (b) inner surface $\langle\cos^2(yJ)\rangle$ values. (c) outer surface 1340 cm^{-1} band heights and (d) inner surface 1340 cm^{-1} band heights.

where the $\langle\cos^2(yY)\rangle$ and $\langle\cos^2(yX)\rangle$ values become approximately equal.

Fig. 4(a) compares the outer and inner surface values of $\langle\cos^2(yY)\rangle - \langle\cos^2(yX)\rangle$, i.e. the difference between the length

and hoop orientation, for the different bottle positions. From this it is clear that the inner surface displays higher levels of hoop orientation throughout although the orientation variation is similar for both surfaces. This arises because the hoop
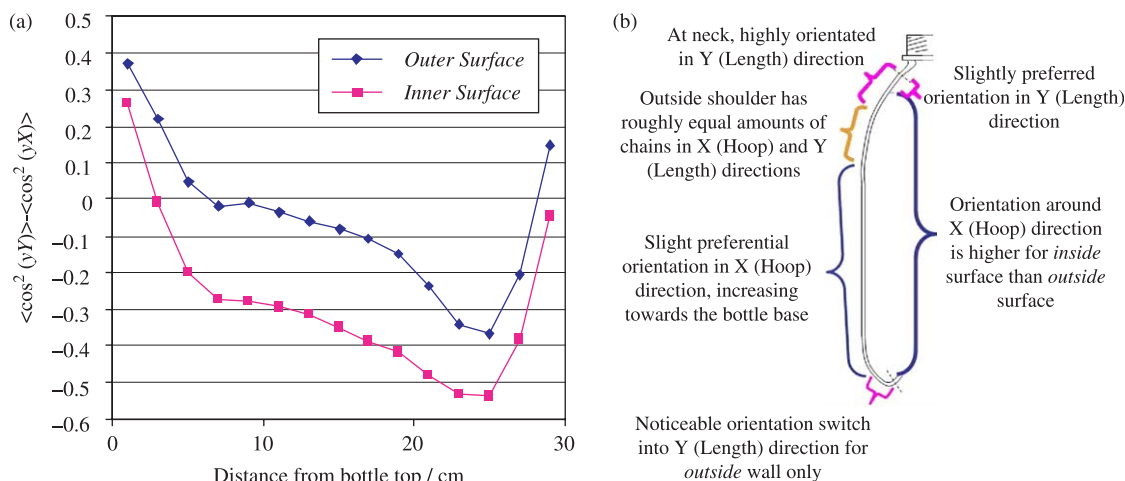

Fig. 4. Chain orientation trends of standard 2*l* stretch-blown PET bottles. (a) $\langle\cos^2(yY)\rangle - \langle\cos^2(yX)\rangle$ values for the inner and outer surfaces along the bottle length. (b) Graphic showing the general chain orientation trends of the outer and inner surfaces.

extension corresponds to a draw ratio of ∼5 for the inner surface, compared to a value of ∼4 for the outer surface [1], as can be seen by considering the dimensions of the preform and final bottle, shown in Fig. 1(a). Indeed, there is a relatively good correlation between the extension of the preform in the length and hoop directions and the corresponding $\langle\cos^2(yJ)\rangle$ values, and this explains why the outline of the $\langle\cos^2(yX)\rangle$ and $\langle\cos^2(yY)\rangle$ curves roughly mimics the 2l bottle shape.

Note that for the most highly oriented surface regions of the inner wall, non-physical, slightly negative values of $\langle\cos^2(yZ)\rangle$ are obtained. Although positive $\langle\cos^2(yZ)\rangle$ values are still within the maximum possible experimental error of 0.14, it may be that an additional normalisation error also arises, since the $1410\ cm^{-1}$ normalisation band has only been tested on films up to draw ratio 4, and the inner wall hoop extension for this region corresponds to a draw ratio of ∼5. However, irrespective of the precise cause for the perturbed $\langle\cos^2(yJ)\rangle$ values at the highest draw ratios, the technique can still be used to compare reliably the relative orientation values for each region of the bottle. These general chain orientation trends are summarised in Fig. 4(b).

Fig. 3(c) and (d) show that the variation in the normalised height measurements of the $1340\ cm^{-1}$ band in the TE_X and TE_Y geometries for the outer and inner bottle surfaces mimics the more thorough $\langle\cos^2(yJ)\rangle$ approach closely. Hence, to a first approximation, the trends in relative chain orientation can be assessed just by considering the orientation of the CH_2 trans conformers.

In contrast to the complex surface chain orientation present within the bottle, the benzene ring orientation at the bottle surface shows very little variation. In particular, Fig. 5 shows that there is a strong tendency for alignment of the plane of the benzene rings parallel to the surface at all bottle positions, since the $\langle\cos^2(zZ)\rangle$ parameter is consistently high at ∼0.6–0.65. This benzene orientation is qualitatively consistent with the surface chains orienting preferentially in the bottle length and hoop directions, since only chains oriented in the bottle thickness direction necessarily cause the benzene ring to align perpendicular to the surface. However, the value of $\langle\cos^2(zZ)\rangle$ is

higher than the 0.5 value expected if all the surface chains were oriented parallel to the surface, with random orientation of the rings about the extended chain axis. So, there is clearly an additional tendency for the benzene rings to align parallel to the surface, presumably because this configuration minimises the surface energy. A similar preferential alignment of the benzene rings has also been observed for spin-coated PET layers [15] and for uniaxially drawn films [16].

3.3. 2l PET bottles with non-standard preform heating times

The effect of altering the preform heating time prior to stretch-blowing was assessed for a series of preforms taken from the same batch, to ensure that they had identical resin molecular weights and isophthalic acid contents. The ideal total preform heating time, t, is 44 s, and the effect of varying this from t minus 20 seconds (Bht-20), to t plus 15 seconds (Bht + 15) in 5 s increments was investigated. The effect of these different preform heating times on bottle optical clarity is shown in Fig. 1(c). Two types of optical clarity deterioration are evident for the Bht + 15 and Bht-20 to Bht-10 bottles. The white opaque regions in the Bht + 15 bottle provide evidence of excess crystallinity forming in the preform prior to the stretch, with the crystalline regions remaining most concentrated at the neck and base regions of the final bottle since these regions have undergone more heating and less stretching. The pearl-like clouding in the Bht-20 to Bht-10 bottles is observed primarily along the bottle's length and not the neck and base regions, and probably results from light scattering on tiny voids that form due to the cooler preform being unable to stretch quickly enough under high draw ratios. This effect was reproduced by cold drawing PET strips on an Instron stretching machine at fast draw rates. Moreover, when clamping the opaque Bht-20 specimens to the ATR element, the clamped regions became transparent, supporting the void hypothesis.

For the bottle blown after $t-20$ s (see Fig. 6), there is a sharp orientation increase in the hoop direction towards the base region, which peaks at 25 cm from the bottle top once more. This is apparent for both the inner and outer surface wall.
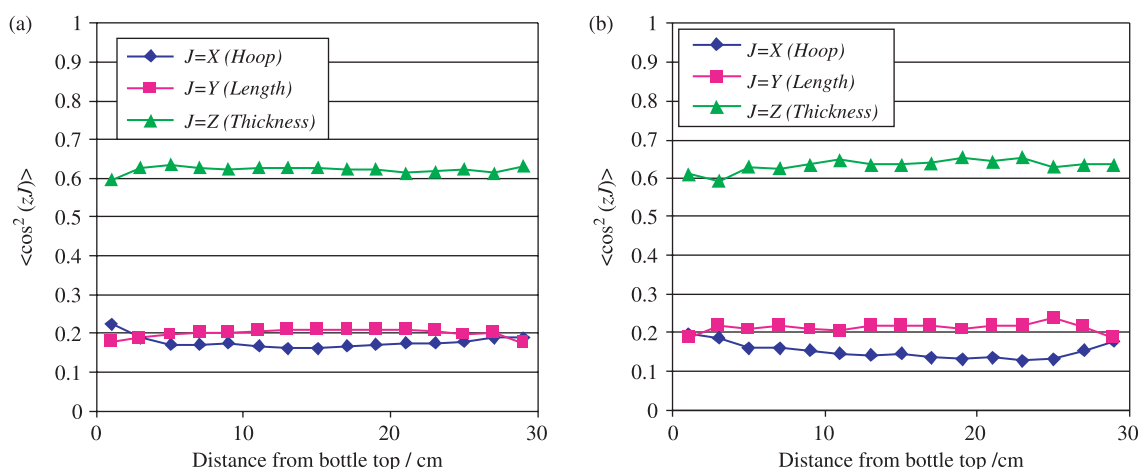

Fig. 5. Benzene ring orientation results for a standard PET bottle (Bht) along the bottle length. (a) Outer surface $\langle\cos^2(zJ)\rangle$ values. (b) inner surface $\langle\cos^2(zJ)\rangle$ values.
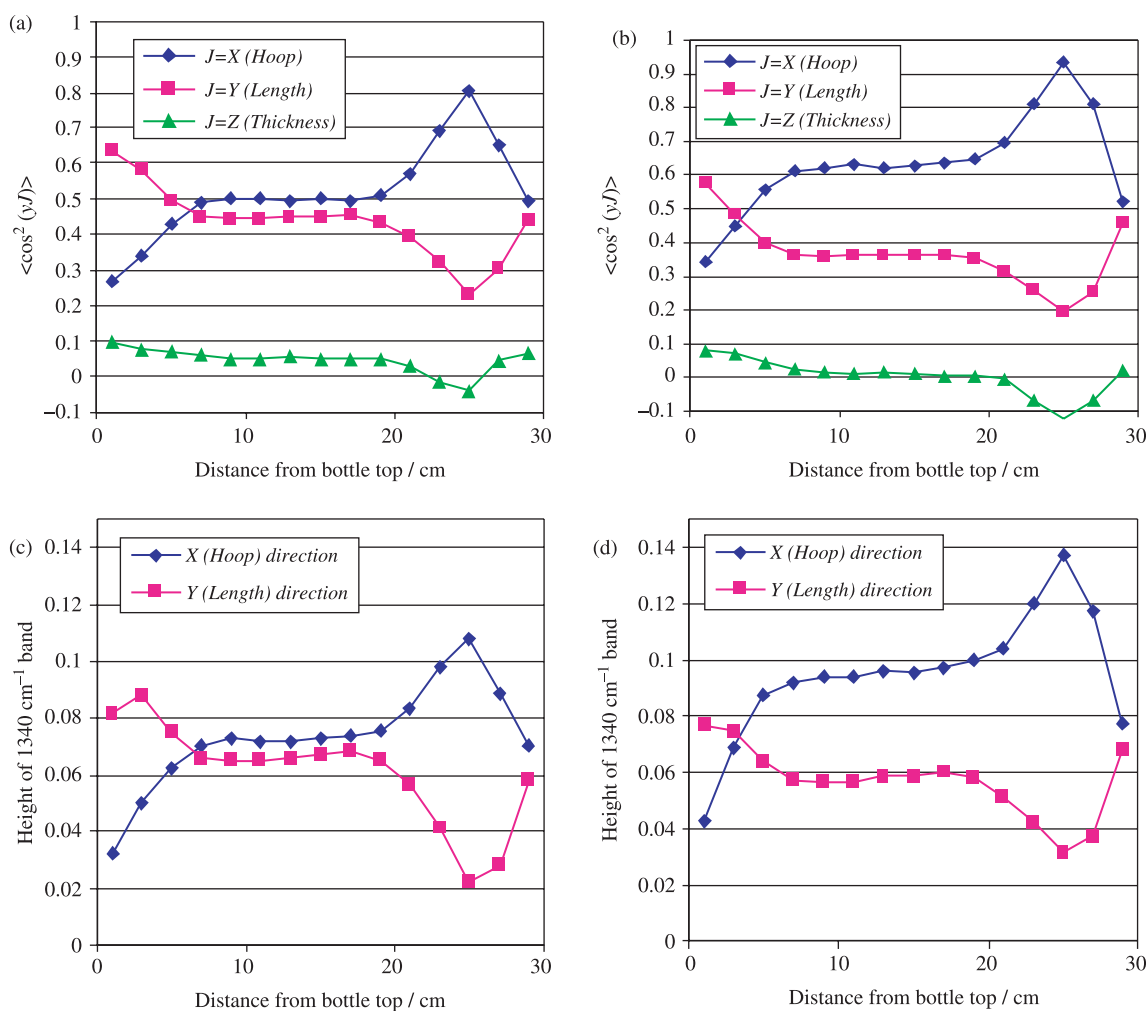
Fig. 6. Chain orientation results along the bottle length for a PET bottle with the ideal preform heating time minus 20 s (Bht-20). (a) Outer surface $\langle\cos^2(yJ)\rangle$ values. (b) inner surface $\langle\cos^2(yJ)\rangle$ values. (c) outer surface 1340 cm^{-1} band heights and (d) inner surface 1340 cm^{-1} band heights.

The minima in the $\langle\cos^2(yY)\rangle$ and $\langle\cos^2(yZ)\rangle$ values at this position are also more pronounced, suggesting that the reduced preform heating times result in less chain orientation relaxation following the stretch blow process and hence greater chain orientation variations. For the Bht-15, Bht-10 and Bht-5 bottles, the orientation trends match those of the standard bottle (Bht) more closely, showing that the deterioration in optical clarity is not matched by altered orientation effects.

As the heating time increases above that of a standard bottle, the surface chain orientation variation along the bottle length reduces. The Bht+5 bottle shows a slight decrease in overall surface orientation compared to the standard (Bht) bottle, although the same general trends are observed. Increasing the preform heating time to $t+10$ s results in even less surface orientation variation in the final product; typical values of $\langle\cos^2(yY)\rangle$ and $\langle\cos^2(yX)\rangle$ along the bottle length are ~ 0.5 and 0.4, respectively, for the outer surface, and ~ 0.6 and 0.4, respectively, for the inner surface. At the neck and base surface regions, though, the $\langle\cos^2(yY)\rangle$ and $\langle\cos^2(yX)\rangle$ values remain similar to those of standard bottle for both surfaces. For the

longest preform heating time of $t+15$ s, Fig. 7 shows that there is noticeably less variation between the $\langle\cos^2(yY)\rangle$ and $\langle\cos^2(yX)\rangle$ values, especially along the outer surface bottle length. In addition, the outer surface neck and base regions, which undergo the longest preform heating times, show particularly low orientation, with the $\langle\cos^2(yZ)\rangle$ values of ~ 0.2 to 0.3 being more similar to the $\langle\cos^2(yY)\rangle$ and $\langle\cos^2(yX)\rangle$ values, whereas at all other positions the $\langle\cos^2(yZ)\rangle$ values remained within the ~ 0–0.1 range found for all the other bottles. The inner bottle surface retains a slight preferential orientation in the hoop direction for much of the bottle length, but towards the base the $\langle\cos^2(yY)\rangle$ and $\langle\cos^2(yX)\rangle$ values become similar. In addition, the maximum in $\langle\cos^2(yX)\rangle$ and minima in $\langle\cos^2(yY)\rangle$ and $\langle\cos^2(yZ)\rangle$ at 25 cm from the bottle top are no longer evident. These findings of reduced chain orientation variation indicate that heating the preform for too long raises the polymer temperature too high above its T_g, so that the hotter polymer flows more readily in response to local stress gradients and so could possibly undergo some flow drawing [17,18] during the stretch blow process and/or
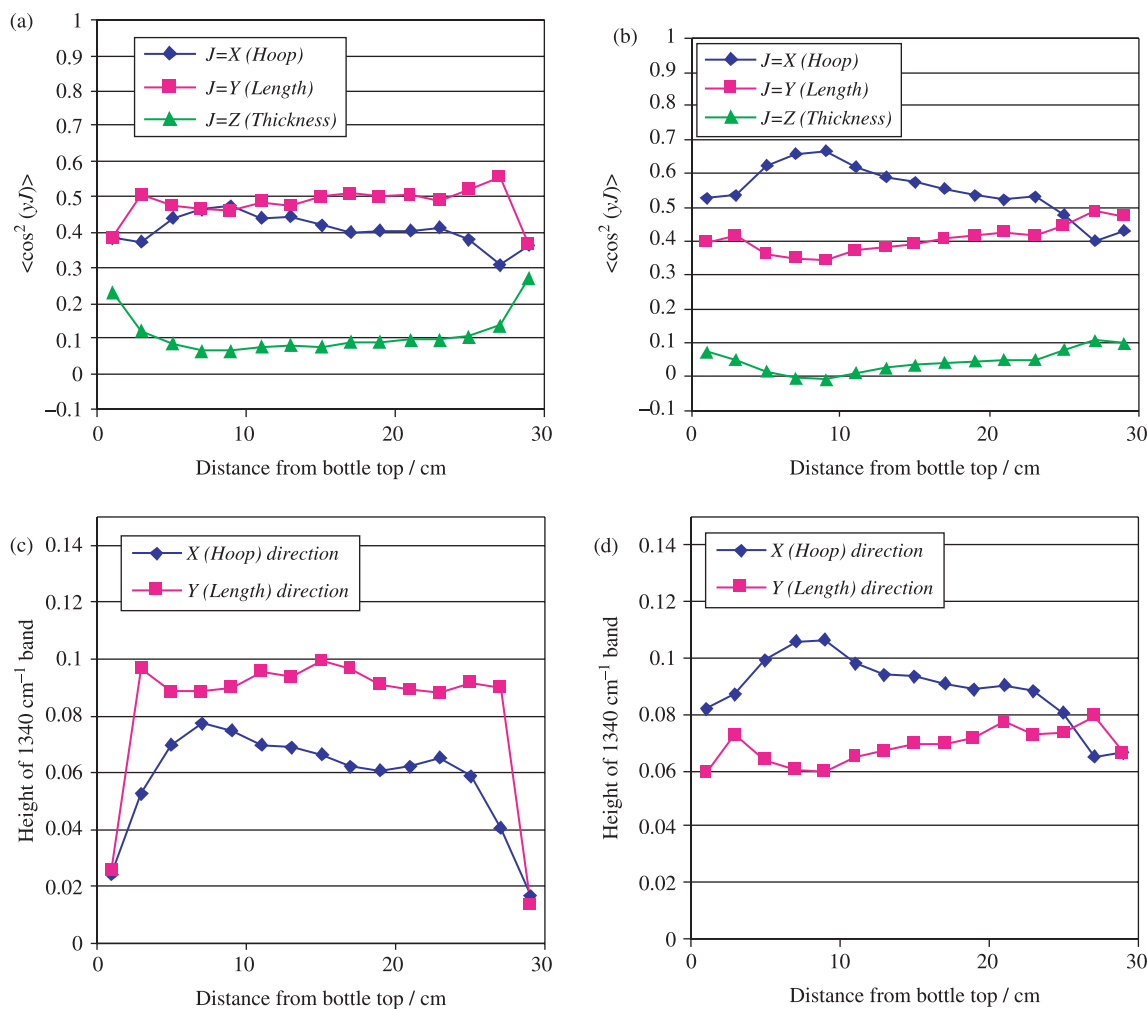
Fig. 7. Chain orientation results along the bottle length for a PET bottle with the ideal preform heating time plus 15 s (Bht + 15). (a) Outer surface $\langle\cos^2(yJ)\rangle$ values. (b) Inner surface $\langle\cos^2(yJ)\rangle$ values. (c) Outer surface 1340 cm^{-1} band heights and (d) inner surface 1340 cm^{-1} band heights.

increased orientational relaxation following this process. Hence, this study reveals that it is important not to heat the preforms for too long before the stretch-blow procedure if high levels of orientation are to be preserved; heating the preform for 5–10 s longer results in decreased orientation without adversely affecting bottle clarity and so such overheated bottles would be difficult to spot in production.

Since, the $\langle\cos^2(yZ)\rangle$ values are consistently low, the surface chain orientation trends can be conveniently visualised by plotting the single parameter $\langle\cos^2(yY)\rangle - \langle\cos^2(yX)\rangle$ for all the bottles, see Fig. 8. The decrease in surface orientation variation for bottles with prolonged preform heating times is clearly evident, as is the increased surface orientation in the hoop direction towards the bottle base for the least heated preform.

The variation in the height measurements of the 1340 cm^{-1} band in the TE$_X$ and TE$_Y$ geometries, across the outer and inner bottle surfaces, was found to mimic closely the $\langle\cos^2(yY)\rangle$ and $\langle\cos^2(yX)\rangle$ curves throughout the series. The 1340 cm^{-1} band probes the CH$_2$ trans-only conformer and so this good correlation probably arises because the gauche isomers that remain after drawing are still largely unoriented [18]. Indeed,

the correlation only became poor for the Bht + 15 outer bottle surface neck and base positions, see Fig. 7, where the combination of lower draw rates and prolonged heating resulted in lower orientation (and hence a higher proportion of the neglected gauche conformers) and excess crystallinity in the form of (presumably) unoriented spherulites, as shown by the bottle clouding in these regions (see Fig. 1(c)). Since, clouding makes the Bht + 15 bottles commercially unviable, anyway, the 1340 cm^{-1} measurements in the TE$_X$ and TE$_Y$ geometries do provide a quicker way of mapping surface orientation trends in commercial PET bottles than the more meticulous $\langle\cos^2(yJ)\rangle$ approach. This may be useful for quality control tests on PET bottles, especially as heating the preform for slightly too long can diminish the orientation without affecting the optical clarity.

For all the bottles the $\langle\cos^2(zZ)\rangle$ parameter remained consistently high at ~0.55–0.65 at all surface bottle positions sampled. The only exception to this occurred for the Bht + 15 bottle neck and base positions where the $\langle\cos^2(zZ)\rangle$ value fell as low as 0.32 showing that the benzene alignment parallel to the surface was significantly reduced. This, however, can be
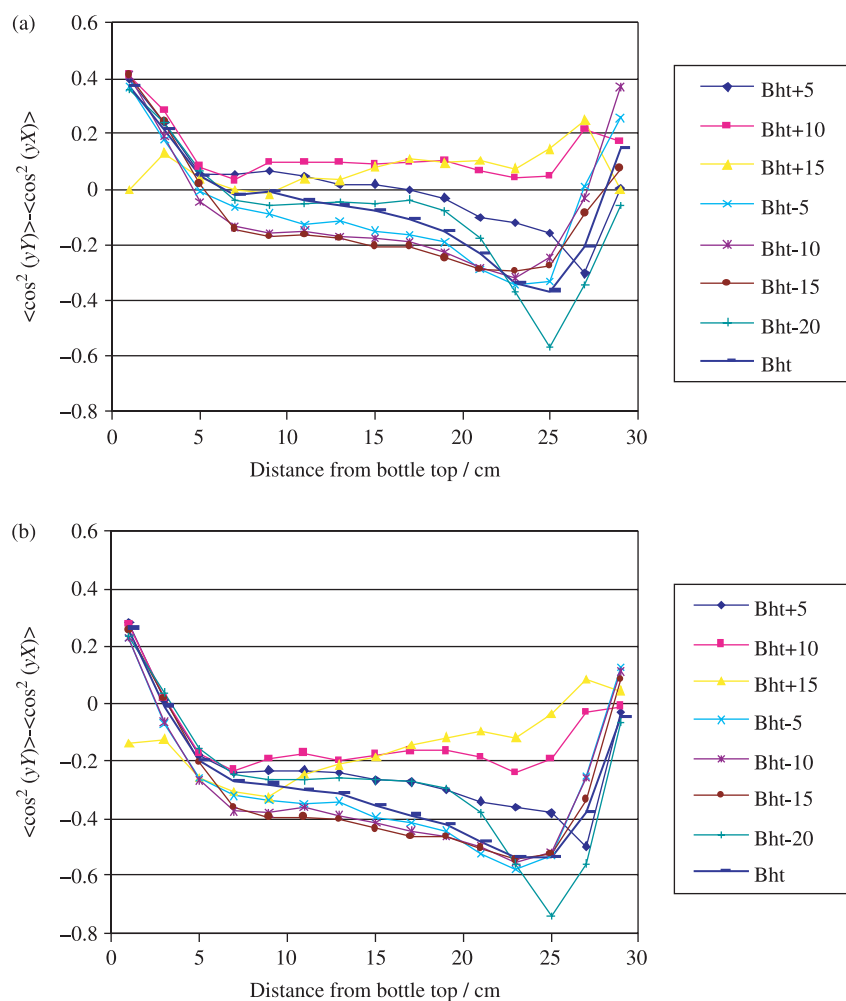
Fig. 8. Summary of chain orientation trends of 2l stretch-blown PET bottles with different preform heating times shown by the $\langle\cos^2(yY)\rangle - \langle\cos^2(yX)\rangle$ values for the (a) inner and (b) outer surfaces along the bottle length.

attributed to the increased number of surface chains lying perpendicular to the surface for this lower oriented region, since the $\langle\cos^2(yZ)\rangle$ values are higher at ~ 0.2–0.3, see Fig. 7(a). Hence again we find that the benzene rings preferentially align parallel to the surface for surface aligned chains.

4. Conclusions

1. The polarised FTIR-ATR technique is a reliable and reproducible method of determining surface orientation trends in PET bottles.
2. The surface chain orientation is uniformly low in the bottle thickness direction at all bottle positions for all the bottles studied; $\langle\cos^2(zZ)\rangle$ values of <0.1 are typical, except when prolonged preform heating resulted in significantly randomised orientation and excess crystallinity. For the standard 2l commercial bottle, the surface chain orientation trends in the bottle hoop and length directions are more complex, but can be broadly summarised as follows. The surface chains lie predominantly in the bottle length direction at the bottle neck,

with the number of chains lying in the hoop direction increasing on moving down the bottle, so that predominantly hoop-direction chains are observed for much of the bottle length. The number of hoop-direction chains reaches a maximum towards the bottle base, after which the number of chains lying in the hoop and length directions becomes more similar. The inner bottle surface shows greater chain orientation in the hoop direction than the outer bottle surface, since the former undergoes a greater expansion in this direction, but the relative trends are similar.

3. Increasing the preform heating times on the standard 2l PET bottles results in significantly less variation in the surface chain orientation, which is attributed to increased chain relaxation effects; bottle clouding is also observed. Decreased preform heating times has a less dramatic effect on surface chain orientation, but can result in bottle clouding.
4. The use of the $1340\ \mathrm{cm}^{-1}$ band absorbencies in the TE_X and TE_Y geometries is a particularly simple and yet accurate method of measuring surface orientation trends in PET for all bottles except those exhibiting excess

crystallinity and low orientation.

5. Preferential alignment of the benzene rings parallel to the surface is observed. This is attributed to the minimum in the surface energy that this conformation provides.

Acknowledgements

References

[1] Everall NJ, Bibby A. Appl Spectrosc 1997;51:1083–91 [Please note the following minor errors, though. The first bracketed term in the P_{222} equation (Eq. (4)) should read $(1+\cos^2\theta)$ rather than $(1-\cos^2\theta)$, and in Eq. (13) the numerator should read $-4n_y n_z \left(1 - n_z^2/n_1^2 \sin^2\theta\right)$ rather than $-4n_y n_z \left(1 - n_x^2/n_1^2 \sin^2\theta\right)$].

[2] See, e.g. (a) Marco Y, Chevalier L, Chaoche M. Polymer 2002;43: 6569–74. (b) Gorlier E, Haudin JM, Billon N. Polymer 2001;42:9541–9.
(c) Goschel U. Polymer 1995;36:1157–65.
(d) Dechampchesnel JBF, Bower DI, Ward IM, Tassin JF, Lorentz G. Polymer 1993;34:763–3770.
(e) Mahendrasingam A, Blundell DJ, Wright AK, Urban V, Narayanan T, Fuller W. Polymer 2003;44:5915–25.
(f) Chaari F, Chaouche M, Doucet J. Polymer 2003;44:473–9.

[3] Everall N, MacKerron D, Winter D. Polymer 2002;43:4217–23.

[4] Matthews RG, Ajji A, Dumoulin MM, Prud'homme RE. Polymer 2000; 41:7139–45.

[5] Guèvremont J, Ajji A, Cole KC, Dumoulin MM. Polymer 1995;36: 3385–92.

[6] Kazarian SG, Brantley NH, Eckert CA. Vib Spectrosc 1999;19:277–83.

[7] Liu C, Jin Y, Zhu Z, Sun Y, Hou M, Wang Z. Nucl Instrum Methods Phys Res B 2000;169:72–7.

[8] Dadsetan M, Mirzadeh H, Sharifi N. Radiat Phys Chem 1999;56: 597–604.

[9] Freure C, Chen G, Horton JH. Surf Sci 1999;437:231–8.

[10] Each $\langle\cos^2(jJ)\rangle$ value is obtained from 4 absorbance measurements, and so the maximum possible error is found by considering every combination of a 10% absorbance error in each measurement. The maximum error in different $\langle\cos^2(jJ)\rangle$ values arises from different combinations, and so we refrain from stating an error for each $\langle\cos^2(jJ)\rangle$ value.

[11] See Jarvis DA, Hutchinson IJ, Bower DI, Ward IM. Polymer 1980;21: 41–54. [The relevant equations can be obtained directly on using $x_1 = x$, $x_2 = z$, $x_3 = y$, $X_1 = X$, $X_2 = Z$ and $X_3 = Y$] .

[12] Jarvis DA, Hutchinson IJ, Bower DI, Ward IM. Polymer 1980;21:41–54.

[13] Walls DJ. Appl Spectrosc 1991;45:1193–8.

[14] See e.g. (a) Flournoy PA, Schaffers WJ. Spectrochim Acta 1966;22: 5–13. (b) Flournoy PA. Spectrochim Acta 1966;22:15.
(c) Mirabella FM. J. Polym Sci, Polym Phys Ed 1984;22:1293–304.
(d) Mirabella FM. Appl Spectrosc 1988;42:1258–65.
(e) Hobbs JP, Sung CSP, Krishnan K, Hill S. Macromolecules 1983;16: 193–9.
(f) Yuan P, Sung CSP. Macromolecules 1991;24:6095–103.
(g) Walls D. Appl Spectrosc 1991;45:1193–8.
(h) Park SC, Liang Y, Lee HS, Kim YH. Polymer 2004;45:8981–8.

[15] Durell M, MacDonald JE, Trolley D, Wehrum A, Jukes PC, Jones RAL, et al. Europhys Lett 2002;58:844–50.

[16] Lapersonne P, Tassin JF, Monnerie L. Polymer 1994;35:2192–6.

[17] Gupta VB, Sett SK, Venkataraman A. Polym Eng Sci 1990;30: 1252–7.

[18] Ajji A, Guèvremont J, Cole KC, Dumoulin MM. Polymer 1996;37: 3707–14.